Toxicology Reports 2 (2015) 1182–1193

Contents lists available at ScienceDirect

Toxicology Reports

journal homepage: www.elsevier.com/locate/toxrep

Inhibitory actions by ibandronate sodium, a nitrogen-containing bisphosphonate, on calcium-activated potassium channels in Madin–Darby canine kidney cells

Sheng-Nan Wu[a,*], Hui-Zhen Chen[a], Yu-Hung Chou[b], Yan-Ming Huang[a], Yi-Ching Lo[c]

[a] Department of Physiology, National Cheng Kung University Medical College, Tainan City, Taiwan
[b] School of Medicine, Mayne Medical School, University of Queensland, Brisbane, Queensland, Australia
[c] Department of Pharmacology, Kaohsiung Medical University, Kaohsiung City, Taiwan

ARTICLE INFO

Article history:
Received 30 June 2015
Received in revised form 23 August 2015
Accepted 25 August 2015
Available online 28 August 2015

Keywords:
Ibandronate
MDCK cell
Large-conductance Ca^{2+}-activated K^+ channel
Intermediate-conductance Ca^{2+}-activated K^+ channel
Membrane potential

ABSTRACT

The nitrogen-containing bisphosphonates used for management of the patients with osteoporosis were reported to influence the function of renal tubular cells. However, how nitrogen-containing bisphosphates exert any effects on ion currents remains controversial. The effects of ibandronate (Iban), a nitrogen-containing bisphosphonate, on ionic channels, including two types of Ca^{2+}-activated K^+ (K_{Ca}) channels, namely, large-conductance K_{Ca} (BK_{Ca}) and intermediate-conductance K_{Ca} (IK_{Ca}) channels, were investigated in Madin–Darby canine kidney (MDCK) cells. In whole-cell current recordings, Iban suppressed the amplitude of voltage-gated K^+ current elicited by long ramp pulse. Addition of Iban caused a reduction of BK_{Ca} channels accompanied by a right shift in the activation curve of BK_{Ca} channels, despite no change in single-channel conductance. Ca^{2+} sensitivity of these channels was modified in the presence of this compound; however, the magnitude of Iban-mediated decrease in BK_{Ca}-channel activity under membrane stretch with different negative pressure remained unchanged. Iban suppressed the probability of BK_{Ca}-channel openings linked primarily to a shortening in the slow component of mean open time in these channels. The dissociation constant needed for Iban-mediated suppression of mean open time in MDCK cells was 12.2 μM. Additionally, cell exposure to Iban suppressed the activity of IK_{Ca} channels, and DC-EBIO or 9-phenanthrol effectively reversed its suppression. Under current-clamp configuration, Iban depolarized the cells and DC-EBIO or PF573228 reversed its depolarizing effect. Taken together, the inhibitory action of Iban on K_{Ca}-channel activity may contribute to the underlying mechanism of pharmacological or toxicological actions of Iban and its structurally similar bisphosphonates on renal tubular cells occurring *in vivo*.

1. Introduction

Bisphosphonates are recognized as stable analogs of pyrophosphates, which have been approved for treatment of postmenopausal osteoporosis [23]. These compounds are not metabolized in either man or animal, and consequently, they are the active, parent compounds. The principal route of their elimination results from renal excretion [15] and these compounds can accumulate in the kidney during therapy [3,38]. It is important to note that potential nephrotoxicity has been observed in patients receiving high-dose bisphosphonate therapy, particularly when administrated by rapid intravenous administration [2,18,22,27–29,32]. The renal effects of these compounds were thought to be through a mechanism linked to their inhibition of farnesyl pyrophosphate synthase [19].

Abbreviations: BKCa channel, large-conductance Ca^{2+}-activated K^+ channel; [Ca2+]i, intracellular Ca2+ concentration; DC-EBIO, 5,6-dichloro-1-ethyl-1,3-dihydro-2H-benzimidazol-2-one; DMEM, Dulbecco's modified Eagle's medium; FBS, fetal bovine serum; H2S, hydrogen sulfide; Iban, ibandronate sodium; IK, voltage-gated K+ current; IKCa channel, intermediate-conductance Ca^{2+}-activated K+ channel; I–V, current–voltage; KCa channel, Ca^{2+}-activated K+ channel; KD, dissociation constant; MDCK cell, Madin–Darby canine kidney cell,NaHS, sodium hydrosulphide; PF573228, 3,4-dihydro-6-[[4-[[[3-(methylsulfonyl)phenyl]methyl]amino]-5(trifluoromethyl)-2-pyrimidinyl]amino]-2(1H)-quinolinone; SEM, standard error of the mean; TRAM-34, 1-((2-chlorophenyl) (diphenyl)methyl)-1H-pyrazole.

* Corresponding author at: Department of Physiology, National Cheng Kung University Medical College. No. 1, University Road, Tainan City 70101, Taiwan. Fax: +886 6 2362780.
E-mail address: snwu@mail.ncku.edu.tw (S.-N. Wu).

http://dx.doi.org/10.1016/j.toxrep.2015.08.010

It has been demonstrated that intermittent treatment with ibandronate (Iban) or zoledronate, which is known to be a potent nitrogen-containing bisphosphonate, caused hypertrophy and hyperplasia of distal tubules and collecting ducts in the rats [29]. Alternatively, previous observations at our laboratory showed that iban was able to decrease the activity of IK_{Ca} channels in RAW 264.7 osteoclast precursor cells and that its block of these channels appeared to have a causal link to the inhibition of cell migration [45]. In contrast, another noteworthy study by Ma et al. [20] has demonstrated that zoledronate could activate the activity of BK_{Ca} channels in breast cancer cells and that such effect appeared to be responsible for the apoptotic change caused by this compound. However, the ionic mechanism of their actions on renal tubular cells remains largely elusive.

The BK_{Ca} channels (maxi-K, $K_{Ca}1.1$, *KCNNMA1*, *Slo1*) are products of a nearly ubiquitous, alternatively spliced gene. They possess the largest single-channel conductance of all K^+ selective channels, which are synergistically activated by membrane depolarization and/or elevation of $[Ca^{2+}]_i$ [43]. These pharmacologically promiscuous channels which can be stimulated by a chemically diverse range of small molecule drugs are functionally expressed in many cell types, including renal tubular cells [5,17,24,37,43,44]. Of importance, these channels are localized in a variety of kidney cells, where they have important roles ranging from regulators of glomerular filtration to conduits for K^+ secretion [17,24,40,41]. However, how Iban can interact with these channels to perturb whole-cell currents or membrane potential is incompletely understood.

Previous studies have reported the important roles of K_{Ca} channels in kidney functions. For example, perfusion of isolated collecting ducts revealed that iberiotoxin, an inhibitor of BK_{Ca} channels, could inhibit K^+ secretion during high tubular fluid flow [42]. Renal responsiveness to consumption of high K, alkaline diet was reported to be seriously impaired in BK-β4 knockout mice and their plasma K^+ level was greatly elevated [9,41]. Additionally, IK_{Ca} channels have been demonstrated to be strongly linked to diabetic nephropathy [10].

The Madin–Darby canine kidney (MDCK) renal tubular cell line has been a useful model for studies of functional activities existing in renal tubular cells [13,14]. Therefore, to fill the knowledge gap, the goals of this study were (1) to investigate possible effects of Iban on macroscopic and single-channel currents and (2) to determine how it can interact with ion channels to modify membrane potential of MDCK cells. Besides its inhibition of farnesyl pyrophosphate synthase [19], the effects of Iban on ion channels shown in this study are obligate mechanisms by which it or its structurally similar bisphosphonates can influence the functional activities of renal tubular cells, if similar findings occur *in vivo*.

2. Materials and methods

2.1. Drugs and solutions

Ibandronate sodium (Iban; $C_9H_{22}NO_7P_2Na \cdot H_2O$; Bonviva®) was obtained from Hoffmann-La Roche Ltd. (Basel, Switzerland), (±)-ketamine was from Cerilliant Corp. (Round Rock, TX), paxilline was from Alomone Labs (Jerusalem, Israel), ionomycin, oxalate (ethanedioate) and sodium hydrosulphide (NaHS) were from Sigma–Aldrich Inc. (St. Louis, MO), DC-EBIO (*i.e.*, 5,6-dichloro-1-ethyl-1,3-dihydro-2*H*-benzimidazol-2-one), and 9-phenanthrol, PF573228 (*i.e.*, 3,4-dihydro-6-[[4-[[[3-(methylsulfonyl) phenyl]methyl]amino]-5(trifluoromethyl)-2-pyrimidinyl]amino]-2(1*H*)-quinolinone) and TRAM-34 (*i.e.*, 1-((2-chlorophenyl) (diphenyl) methyl)-1*H*-pyrazole) were from Tocris (Bristol, UK). Chlorotoxin was kindly provided by Dr. Woei-Jer Chuang (Department of Biochemistry, National Cheng Kung University Medical College, Tainan City, Taiwan). All culture media, FBS, L-glutamine, penicillin-streptomycin, fungizone and trypsin/EDTA were obtained from Invitrogen (Carlsbad, CA). All other chemicals were commercially available and of reagent grade. Twice-distilled water was de-ionized through a Milli-Q water purification system (APS Water Services Inc., Van Nuys, CA).

The composition of the bathing solution (*i.e.*, normal Tyrode's solution) was 136.5 mM NaCl, 5.4 mM KCl, 1.8 mM $CaCl_2$, 0.53 mM $MgCl_2$, 5.5 mM glucose, and 5.5 mM HEPES-KOH buffer, pH 7.4. To measure K^+ currents or membrane potential in MDCK cells, the patch pipette was filled with a solution consisting of 130 mM K-aspartate, 20 mM KCl, 1 mM KH_2PO_4, 1 mM $MgCl_2$, 3 mM Na_2ATP, 0.1 mM Na_2GTP, 0.1 mM EGTA, and 5 mM HEPES-KOH buffer, pH 7.2.

For the recordings of BK_{Ca}-channel activity, high K^+-bathing solution contained 145 mM KCl, 0.53 mM $MgCl_2$, and 5 mM HEPES-KOH buffer (pH 7.4), and the pipette solution contained 145 mM KCl, 2 mM $MgCl_2$, and 5 mM HEPES-KOH (pH 7.2). The free Ca^{2+} concentration was calculated assuming a dissociation constant of 0.1 mM for EGTA and Ca^{2+} (at pH 7.2) (http://maxchelator.stanford.edu/CaEGTA-TS.htm).

2.2. Cell preparation

The MDCK cell line (BCRC-60004), a canine renal tubular cell line, was obtained from Bioresource Collection and Research Center (Hsinchu, Taiwan). Cells were routinely cultured in DMEM supplemented with 10% heat-inactivated FBS, 100 U/ml penicillin and 100 μg/ml streptomycin at 37 °C in 5% CO_2-containing humidified air [13]. Culture medium was continuously replaced every 2 days to maintain a healthy cell population. For long-term storage, the cells were frozen in DMEM containing 10% dimethyl sulfoxide, and kept in liquid nitrogen. Prior to their use in electrophysiological experiments, cells were grown on glass coverslips in DMEM, in order to have good cell-substrate attachment. Cell viability was commonly evaluated using a WST-1 cell proliferation assay and an ELISA reader (Dynatech, Chantilly, VA). A Nikon Eclipse Ti-E inverted microscope (Li Trading Co., Taipei City, Taiwan) equipped with 5-megapixel cooled digital camera was commonly used to observe cell growth.

2.3. Intracellular Ca^{2+} ($[Ca^{2+}]_i$) measurements of MDCK cells

Cells were loaded with 4 μM fura-2/AM (Molecular Probes, Eugene, OR) for 45 min at room temperature (20–25 °C). Changes in $[Ca^{2+}]_i$ were monitored with single-cell imaging using a TillvisION imaging system equipped with a Polychrome II high-speed monochromator (TILL Photonics, Martinsried, Germany). Fura-2 was excited sequentially by 340 and 380 nm light delivered from a xenon lamp *via* a ×40, 1.3 NA UV fluor oil objective (Olympus, Tokyo, Japan). The fluorescent images were collected at 510 nm scale every 0.5 sec by a Peltier-cooled CCD camera. The ratio of fluorescence, R (340 nm/380 nm), from an individual cell was obtained by using TILL visION software 4.0 (Till Photonics) [47].

2.4. Electrophysiological measurements

Shortly before the experiments, a coverslip, on which MDCK cells were grown, was placed on the home-made recording chamber which was mounted on the stage of a CKX-41 inverted fluorescent microscope (Olympus, Tokyo, Japan) coupled to digital video system (DCR-TRV30; Sony, Japan) with a magnification of up to 1500×. The examined cells were immersed at room temperature (20–25 °C) in normal Tyrode's solution. The electrodes used were pulled from Kimax-51 capillaries (#34500; Kimble Glass, Vineland, NJ) in either a PP-83 puller (Narishige, Tokyo, Japan) or a P-97 Flaming/Brown micropipette puller (Sutter, Novato, CA),

and their tips were fire-polished with an MF-83 microforge (Narishige). The pulled electrodes, which commonly had a tip resistance of 3–5 MΩ when filled with different internal solutions described above, were maneuvered using a WR-98 micromanipulator (Narishige). An anti-vibration air table was used to enhance stability during electrophysiological experiments. Patch clamp recordings were obtained in cell-attached, inside-out or whole-cell configuration using an RK-400 (Bio-Logic, Claix, France) or Axopatch 200B (Molecular Devices, Sunnyvale, CA) amplifier [45]. The junctional potentials between the pipette solution and extracellular medium were corrected immediately before seal formation was made.

To induce membrane stretch, membrane tension of MDCK cells was altered by applying negative pressure with a calibrated syringe to the back end of the recording electrode through the suction port of the electrode holder [5]. Negative pressure was monitored with a pressure manometer (PM01R; World Precision Instruments, Sarasota, FL).

2.5. Data recordings and analyses

Data acquisition and analyses were controlled by pCLAMP 10.2 (Molecular Devices). Current signals were low-pass filtered at 1 or 3 kHz. The data were sampled online in an ASUSPRO-BU401LG laptop computer (ASUS, Taipei City, Taiwan) at 10 kHz. With the aid of a digital-to-analog conversion, the voltage profiles with either rectangular or ramp pulses created from pCLAMP 10.2 were utilized to correctly determine current–voltage (*I–V*) relationships for ion currents (*e.g.*, I_K). The digital data achieved during the experiments were appropriately analyzed by various analytical tools, including Origin 8.0 (OriginLab, Northampton, MA), LabChart 7.0 (PowerLab Software; AD Instruments, KYS Technology Co., Ltd., New Taipei City, Taiwan), and custom-made macros built in an Excel 2013 spreadsheet run on Windows 8 (Microsoft, Redmond, WA).

2.6. Single-channel analyses

The amplitudes of single BK_{Ca}- or IK_{Ca}-channel currents seen in MDCK cells were analyzed by use of pCLAMP 10.2 (Molecular Devices). Multi-gaussian adjustments of the amplitude distributions among channels were commonly created to ensure the existence of single-channel events. The functional independence among channels was verified by comparing the observed stationary probability with the values calculated according to the fitted Gaussian function embedded in pCLAMP 10.2. The channel open probabilities were determined using an iterative process to minimize the x^2 values which were calculated as there were an adequately large number of independent observations. Open and closed-time histograms of BK_{Ca} channels obtained with or without addition of different Iban concentrations were determined by two-exponential function (*i.e.*, fast and slow components). The single-channel conductance of BK_{Ca} or IK_{Ca} channels was calculated by a linear regression using mean single-channel amplitudes given at different levels of voltage.

The effect of Iban on the probability of BK_{Ca}-channel openings seen in MDCK cells are explained by a state-dependent blocker, because this compound preferentially binds to the open state of the channel according to minimal kinetic scheme:

$$C \underset{\beta}{\overset{\alpha}{\rightleftarrows}} O \underset{k_{-1}}{\overset{k_{+1}}{\rightleftarrows}} O \times B$$

where α and β are the rate constants for the opening and closing of BK_{Ca} channels, k_{+1} and k_{-1} are the forward (blocking) and backward (unblocking) rate constants caused by the presence of Iban, and [*B*] is the Iban concentration. C, O and O × B shown in the scheme indicates the closed (resting), open, and open-blocked states, respectively.

On the basis of this reaction scheme, the blocking and unblocking rate constants, k_{+1} and k_{-1}, were determined from the slow component in the open time of BK_{Ca} channels measured at the level of +50 mV. Blocking and unblocking rate constants were then determined using the relation:

$$\frac{1}{\tau_b} = k_{+1} \times [B] + k_{-1}$$

where k_{+1} and k_{-1} are respectively derived from the slope and the *y*-axis intercept at [*B*] = 0 of the linear regression interpolating the reciprocal time constant ($1/\tau_b$) *versus* different Iban concentrations. According to this relation, the linearized plot of $1/\tau_b$ against [*B*] (*i.e.*, the Iban concentration) was obtained (Fig. 3A) and the dissociation constant ($K_D = k_{-1}/k_{+1}$) of Iban can be thereafter generated.

To assess effects of Iban on the activation curve of BK_{Ca} channels, the channel opening probabilities at the different levels of holding potential were measured. The relationships between the membrane potential and the relative open probability obtained before and after addition of Iban (10 μM) were fitted with a Boltzmann function of the following form:

$$\frac{(N \times P)}{(N \times P)_{max}} = \frac{1}{1 + \exp\left[\frac{-(V - V_{1/2})qF}{RT}\right]}$$

where $(N \times P)_{max}$ measured at the level of +90 mV in the control was the taken to be 1.0, $V_{1/2}$ is the voltage at which there is half-maximal activation, *q* the apparent gating charge, *F* Faraday's constant, *R* the universal gas constant, and *T* the absolute temperature.

2.7. Statistical analyses

Linear or nonlinear curve-fitting to experimental data in this study was carried out by means of either pCLAMP 10.2, Microsoft Excel 2013 or Origin 8.0 (OriginLab Corp.). The data of macroscopic or single-channel currents were presented as the mean values ± standard error of the mean (SEM) with sample sizes (*n*) representing the cell number from which the data were taken. The paired or unpaired Student's *t*-test were initially used for the statistical analyses. Assuming that statistical difference among different groups is necessarily evaluated, post-hoc Duncan multiple comparisons were further implemented. Statistical analyses were performed using the Statistical Package for Social Science 20 (SPSS; IBM Corp., Armonk, New York). A *P* value of less than 0.05 was considered to indicate statistical difference.

3. Results

3.1. Inhibitory effect of Iban on voltage-gated K^+ current (I_K) recorded from MDCK cells

In an initial set of electrophysiological experiments, we evaluated the effect of Iban on I_K in these cells under whole-cell current recordings. As MDCK cells grown on a coverslip were immersed in normal Tyrode's solution containing 1.8 mM $CaCl_2$, the I_K in response to a 1 s ramp pulse from −100 to +60 mV could be readily elicited at a rate of 0.05 Hz. When cells were exposed to different concentrations of Iban, the I_K amplitude elicited by the 1 s long ramp pulse became progressively decreased (Fig. 1). For example, at the level of +40 mV, Iban at a concentration of 30 μM reduced current amplitude by 66.2 ± 2.3% from 785 ± 58 to 265 ± 23 pA ($n = 17$, $P < 0.05$). After washout of Iban, I_K amplitude at the same level returned to 626 ± 34 pA ($n = 11$). Similar to Iban effects, paxilline or ketamine effectively suppressed the I_K amplitude. Moreover, a

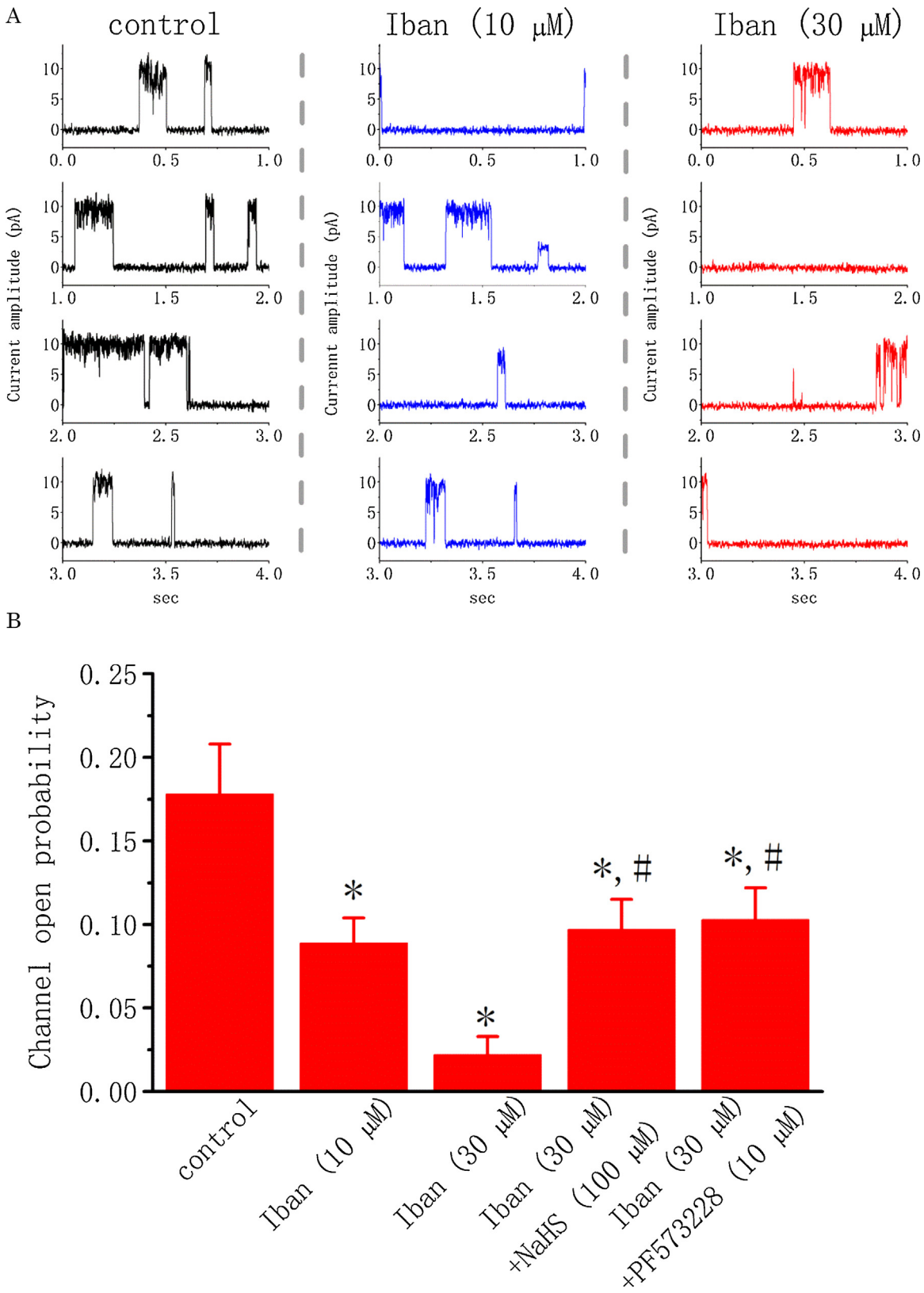

Fig. 2. Effect of Iban on BK_{Ca}-channel activity in MDCK cells. These experiments were conducted as cells were bathed in high-K^+ (145 mM) solution containing 1.8 mM $CaCl_2$. Cell-attached current recordings were made and each cell was held at +50 mV. Followed by standardization with Iban (30 μM), Iban along with NaHS (Iban + NaHS) and PF573228 (Iban + PF573228) were also monitored for the alteration on BK_{Ca}-channel activity which was measured at the level of +50 mV. (A) Original current traces obtained with or without addition of Iban at +50 mV. control (left, black); 10 μM Iban (middle, blue) and 30 μM Iban (right, red). (B) Summary of the data showing effects of Iban, Iban plus NaHS and Iban plus PF573228 on the channel open probability. Values are means ± SEM for $n = 16–18$ cells in each group. *Significantly different from control ($P < 0.05$) and #significantly ($P < 0.05$) different from Iban (30 μM) alone. (For interpretation of the references to color in this figure legend, the reader is referred to the web version of this article.)

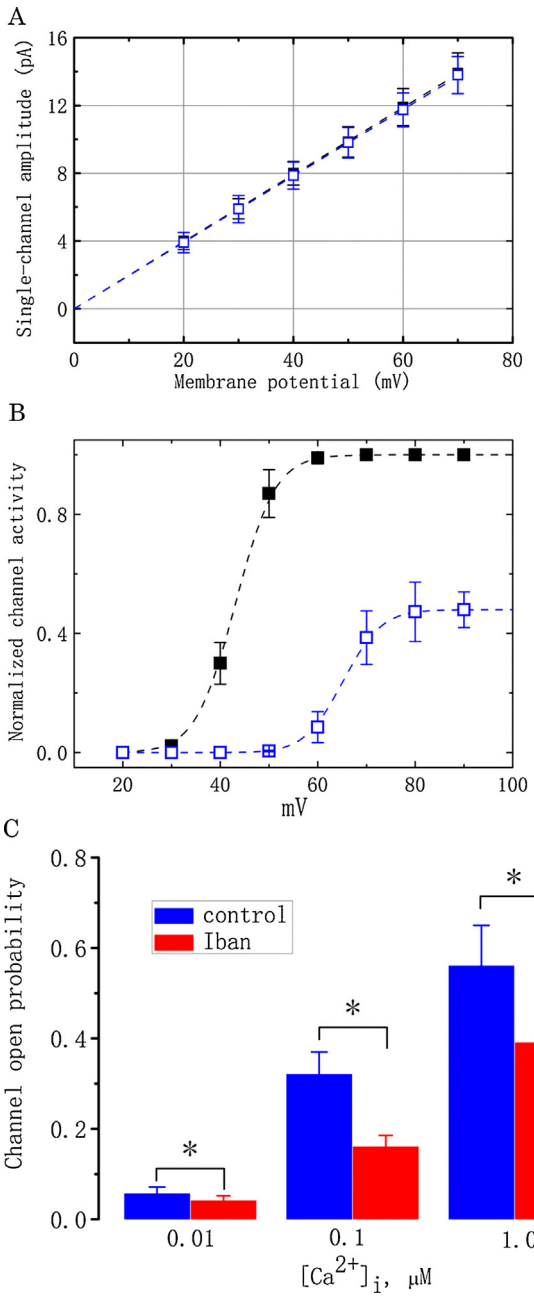

Fig. 3. Effect of Iban on BK_{Ca}-channel activity at different potentials in MDCK cells. For this purpose, cells were exposed to high-K^+ solution containing 1.8 mM $CaCl_2$ and held at different levels of membrane potentials. (A) The *I–V* relationships of BK_{Ca} channels obtained in the absence (■) and presence (□) of 10 μM Iban. Values are means ± SEM for n = 15–18 cells in each point). (B) The relationships between normalized channel activity and membrane potential obtained before and after addition of 10 μM Iban. Values are means ± SEM for n = 12–15 cells in each point. ■: control (black); □: in the presence of 10 μM Iban (blue). (C) Iban (10 μM)-induced Inhibition of BK_{Ca}-channel activity at various concentrations of internal Ca^{2+}. In this set of experiments, inside-out current recordings were performed and different concentrations (0.01, 0.1 and 1 μM) of Ca^{2+} in the bath before (blue bars) and after 10 μM Iban (red bars) were applied to the bath. Values are means ± SEM for 6–8 cells in each group. *Significantly different from controls (P < 0.05). (For interpretation of the references to color in this figure legend, the reader is referred to the web version of this article.)

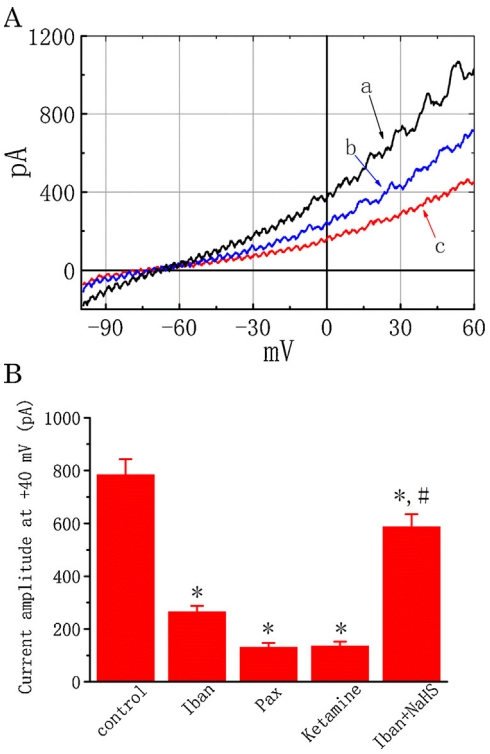

Fig. 1. Effect of Iban on I_K recorded from MDCK cells. (A) Original current traces obtained with or without addition of Iban at −50 mV and a long ramp pulse from−100 to +60 mV with a duration of 1 s at a rate of 0.05 Hz. a: control (black); b: 10 μM Iban (blue); c: 30 μM Iban (red). (B) Summary of the data showing effects of Iban, paxilline, ketamine and Iban plus NaHS on the I_K amplitude measured at the level of +40 mV. Values are means ± SEM for n = 15–18 cells for each group. Iban: 30 μM Iban; Pax: 1 μM paxilline; Ketamine: 100 μM ketamine; NaHS: 100 μM sodium hydrosulfide. *Significantly different from control (P < 0.05) and #significantly (P < 0.05) different from Iban (30 μM) alone. (For interpretation of the references to color in this figure legend, the reader is referred to the web version of this article.)

further addition of soldium hydrosulfide (NaHS, 100 μM) significantly reversed Iban-induced reduction of I_K amplitude elicited by the ramp pulse (Fig. 1B). Paxilline or ketamine are recognized as inhibitors of BK_{Ca} channels [11,43], while NaHS which can release hydrogen sulfide (H_2S) was reported to activate the activity of BK_{Ca} channels [5]. Chlorotoxin (1 μM), a blocker of chloride channels, exerted no effects on I_K in these cells. The observed effect of Iban on macroscopic I_K did not appear to involve in the suppression of Cl^- channels. As such, the results suggest that Iban has a suppressive effect on I_K in these cells.

3.2. *Iban suppressed BK_{Ca}-channel activity measured from MDCK cells*

A considerable mix of different K^+ channels could be measured during whole-cell recordings. For this reason, in order to determine how Iban can interact with ion channels to depress I_K amplitude, single-channel current recordings were performed. In this set of experiments, cell-attached configuration was made and cells were bathed in high K^+ solution containing 1.8 mM $CaCl_2$. As shown in Fig. 2, under our experimental conditions, the activity of BK_{Ca} channels can be readily detected, as described previously in different types of cells [5,24,41]. As Iban at a concentration of 10 or 30 μM was applied to the bath, channel activity was progressively diminished (Fig. 2). For example, addition of Iban (10 μM) significantly reduced the probability of BK_{Ca}-channel openings by 50.1 ± 2.1% from 0.178 ± 0.030 to 0.089 ± 0.015 (n = 18, P < 0.05). Similar to the effect of Iban, paxilline (1 μM) or ketamine (10 μM) applied to the bath was effective at suppressing channel activity. Moreover, in continued presence of 30 μM Iban, further addition of NaHS (100 μM) or PF573228 (10 μM) reversed Iban-mediated

inhibition of BK_{Ca} channels as evidenced by a significant increase in channel activity to 0.097 ± 0.018 (n = 16, P < 0.05) or 0.103 ± 0.019 (n = 16, P < 0.05), respectively. PF573228 was previously reported to activate BK_{Ca} channels [37]. These results indicate that Iban can suppress BK_{Ca}-channel activity in a concentration-dependent manner in MDCK cells.

3.3. Inability of Iban to alter single-channel conductance

The next set of experiments was conducted to determine Iban effects on BK_{Ca}-channel activity measured at different voltages. Cells were bathed in high-K^+ solution, which contained 1.8 mM $CaCl_2$ and the recording pipette was filled with K^+-containing solution. The activity of BK_{Ca} channels was readily detected at different levels of membrane potential. As expected, when membrane became depolarized, the channel open probability continued to increase [43]. As shown in Fig. 3A, according to an ohmic I–V relation of BK_{Ca} channels, no notable difference in the single-channel conductance of these channels recorded from MDCK cells was demonstrated (198 ± 12 pS [control] *versus* 196 ± 11 pS [10 μM Iban], n = 15, P > 0.05), despite a considerable suppression of BK_{Ca}-channel activity during exposure to Iban. It is thus clear from these results that Iban did not have any effects on single-channel conductance of these channels.

3.4. Iban-induced shift in the activation curve of BK_{Ca} channels

Another set of experiments was further performed to examine whether there is voltage dependence for the inhibitory effect of Iban on BK_{Ca}-channel activity. Fig. 3B shows the activation curve of BK_{Ca} channels obtained with or without addition of 10 μM Iban. The relationships between the membrane potentials and the probability of BK_{Ca}-channel openings were derived and thereafter fitted to a Boltzmann function described in Materials and Methods. In control, $V_{1/2}$ = 43.1 ± 1.9 mV and q = 7.1 ± 0.2 e (n = 15), whereas in the presence of 10 μM Iban, $V_{1/2}$ = 65.2 ± 2.2 mV and q = 7.3 ± 0.2 e (n = 12); therefore, addition of Iban not only produced a decrease in the maximal open probability of BK_{Ca} channels, but also significantly shifted the activation curve to a positive membrane potential by approximately 22 mV. In contrast, there was no significant difference in the gating charge of the activation curve between the absence and presence of Iban. These data indicate that, in addition to the reduction of BK_{Ca}-channel activity, Iban is able to produce a rightward shift in the activation curve of BK_{Ca} channels in MDCK cells.

3.5. Change in the magnitude of Iban-mediated reduction of BK_{Ca}-channel activity in different level of internal Ca^{2+}

It was also determined whether Iban can modify the Ca^{2+} sensitivity of BK_{Ca} channels. In this set of experiments, inside-out current recordings were made and different concentrations of Ca^{2+} in the bath before and after addition of Iban (10 μM) to an intracellular surface of the excised patch was applied. At a given concentration of Iban (10 μM), the magnitude of its reduction in BK_{Ca}-channel activity became notably decreased as internal Ca^{2+} was elevated (Fig. 3C). For example, at the holding potential of +50 mV, Iban (10 μM) reduced the activity of BK_{Ca} channels at internal Ca^{2+} concentration of 0.1 μM by 50%, while it at the same concentration decreased channel activity at internal Ca^{2+} concentration of 1 μM only by 30%. Therefore, these data indicated that the presence of Iban was able to alter Ca^{2+} sensitivity of BK_{Ca} channels in MDCK cells.

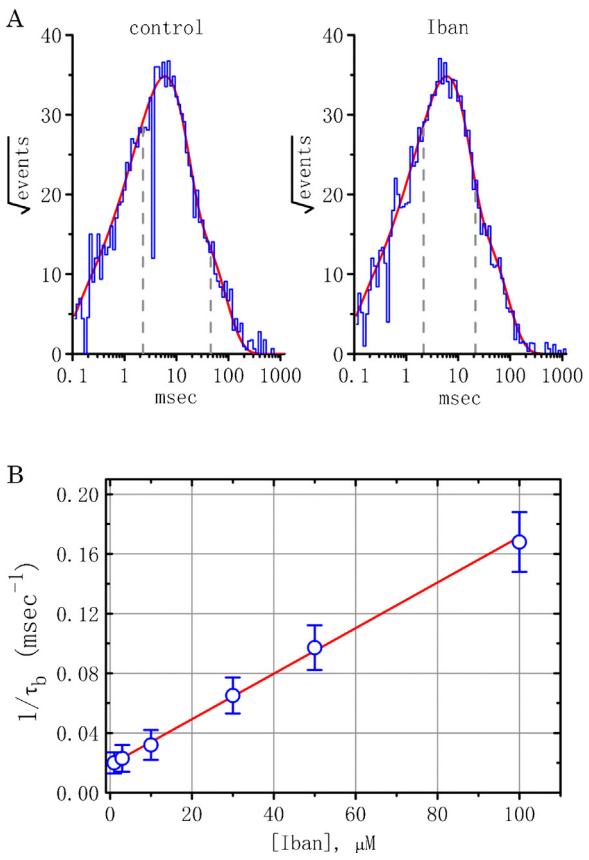

Fig. 4. Effect of Iban on the kinetic properties of BK_{Ca} channels in MDCK cells. (A) Mean open-time histograms of BK_{Ca} channels in the absence (left) and presence (right) of 10 μM Iban. Cells were bathed in high K^+ solution containing 1.8 mM $CaCl_2$ and cell-attached current recordings was made with a holding potential of +50 mV. The abscissa and ordinate shown in each histogram respectively indicate the logarithm of open time (ms) and the square root of the event number. The gray dashed lines shown in each lifetime distribution are placed at the values of time constant (*i.e.*, fast and slow components) in the open state, and the red smooth curves were well fitted by a two-exponential function. Data in the control were obtained from a measurement of 431 channel openings with a total record time of 30 s, whereas those during exposure to Iban (10 μM) were obtained from 480 channel openings with a total record time of 1 m. In (B), the kinetics of Iban-induced reduction in the slow component of mean open time of BK_{Ca} channels was determined. The reciprocal of time constant ($1/\tau_b$) was derived and plotted against the Iban concentration. Data points were fitted by a linear regression, indicating that Iban-mediated reduction of mean open time occurs with a molecularity of 1. Blocking (k_{+1}) and unblocking (k_{-1}) rate constants derived from different Iban concentrations were 0.00153 ms^{-1} μM^{-1} and 0.0187 ms^{-1}, respectively. Each point represent the mean ± SEM (n = 9–12). (For interpretation of the references to color in this figure legend, the reader is referred to the web version of this article.)

3.6. Evaluation of Iban-induced decrease in the slow component of mean open time of BK_{Ca} channels in MDCK cells

Since Iban-induced decrease of BK_{Ca}-channel activity tends to arise notably from a reduction in channel open probability rather than the decreased number of active channels, effects of Iban on the kinetic behavior of BK_{Ca} channels were further analyzed. As shown in Fig. 4A, in cell-attached patches of control cells (*i.e.*, in the absence of Iban), the distribution of open-time durations of BK_{Ca} channels measured at the level of +50 mV was convincingly fit by a two-exponential equations with a mean open time of 2.3 ± 0.1 and 45.6 ± 5.6 msec (n = 12). Particularly, during exposure to 10 μM Iban, the mean duration of the slow components of open-time distribution was drastically shortened. For example, Iban at a concentration of 10 μM significantly decreased the slow component of mean open time to 21.5 ± 2.5 ms (n = 12, P < 0.05), while no significant change in the fast component of mean open time was

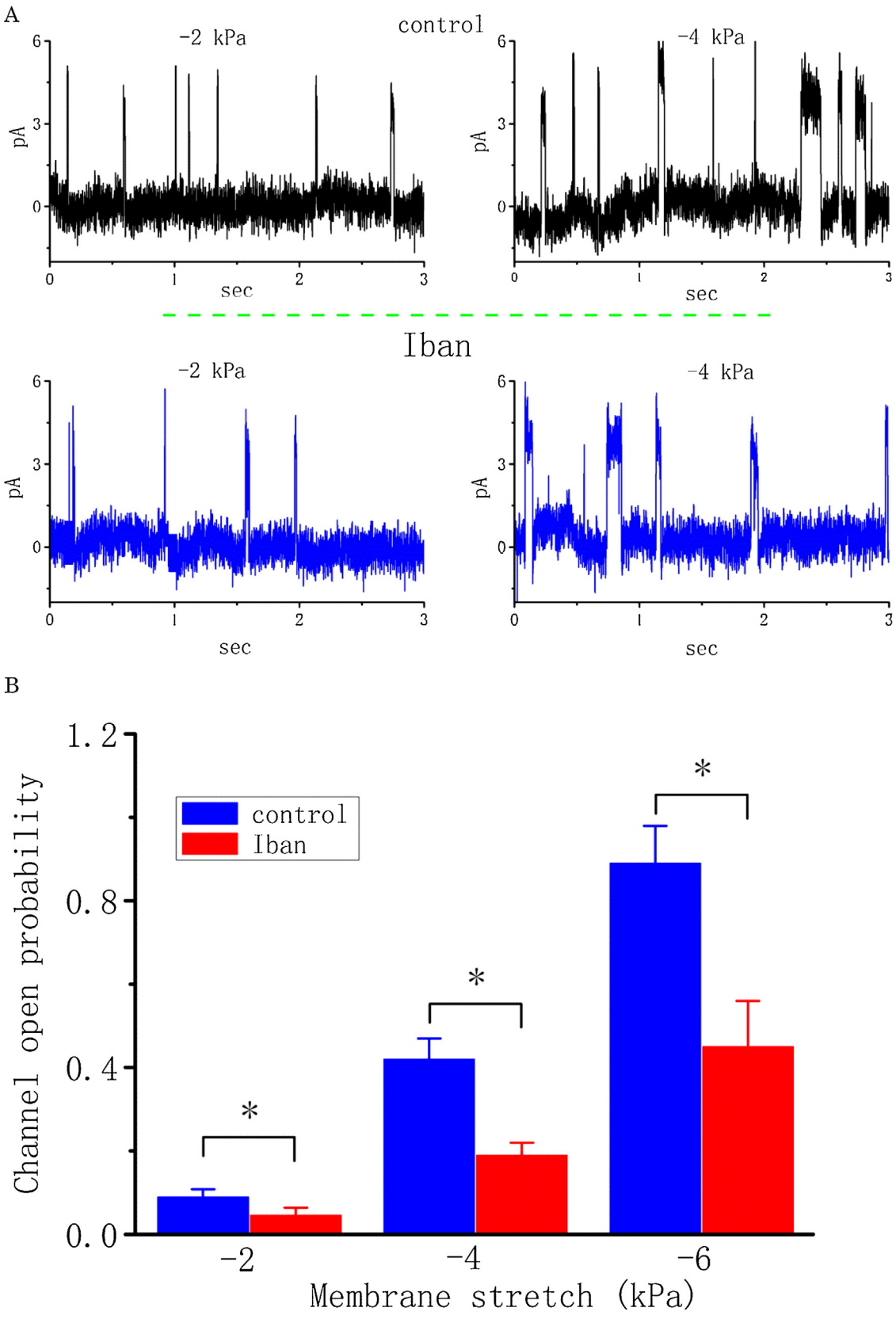

Fig. 5. Effect of membrane stretch on Iban-mediated inhibition of BK_{Ca}-channel activity in MDCK cells. Cells were bathed in high K^+ solution containing 1.8 mM $CaCl_2$. The experiments were conducted in cell-attached configuration with a holding potential of +30 mV. (A) Original current traces showing Iban-induced reduction of BK_{Ca}-channel activity obtained before (upper, black) and after (lower, blue) the membrane stretch induced by a negative pressure (−2 and −4 kPa). Upward deflections are the opening events of the channels. (B) Bar graph showing effects of negative pressure(−2 and −4 kPa) on BK_{Ca} channels in the absence (blue bars) and presence of 10 μM Iban (red bars). Values are means ± SEM for n = 7–10 cells in each group. *Significantly different from controls ($P < 0.05$). (For interpretation of the references to color in this figure legend, the reader is referred to the web version of this article.)

seen (2.2 ± 0.2 ms [n = 12], P > 0.05). The data can be interpreted to mean that Iban-mediated reduction of BK_{Ca} channels is primarily attributable to the shortening of mean open time, despite the fact that it fails to modify single-channel conductance of these channels.

During exposure to Iban, in addition to the decreased probability of BK_{Ca}-channel openings, the slow component of mean open time for BK_{Ca} channels became shortened. To provide more evidence for Iban-induced reduction of BK_{Ca}-channel activity, the time constants for the slow component of mean open time obtain in different Iban concentrations were quantitatively analyzed in this study. Interestingly, the effect of Iban on BK_{Ca} channels in MDCK cells were found to result in a concentration-dependent shortening in the slow component of mean open time (Fig. 4B). According to the first-order blocking scheme described in Materials and Methods, the relationship between $1/\tau_b$ and [B] became linear with correlation coefficient of 0.96 (Fig. 4B). The resultant rate constants of blocking and unblocking perturbed by the presence of Iban were 0.00153 ms^{-1} μM^{-1} and 0.0187 ms^{-1}, respectively. Dividing k_{-1} by k_{+1} is equal to 12.2 μM, a value for the dissociation constant (K_D).

3.7. Effect of membrane stretch on Iban-mediated reduction of BK_{Ca}-channel activity

It has been demonstrated that fluid flow or shear force may alter the activity of BK_{Ca} channels or $[Ca^{2+}]_i$ in renal tubular cells [13,17,31]. Previous reports have shown the ability of membrane stretch to enhance BK_{Ca}-channel activity [5,36,43,44]. We next determined whether Iban effects on these cells can be altered during different level of membrane stretch. It is noted that as an abrupt suction (−2 or −4 kPa) was applied to the membrane, the probability of BK_{Ca}-channel openings became raised (Fig. 5). As such, in MDCK cells, application of membrane stretch can enhance the activity of BK_{Ca} channels, although this maneuver actually did not modify single-channel conductance. Findings from these results thus led us to suggest that the BK_{Ca} channel may in part account for stretch- or flow-induced cellular effects in renal tubular cells *in vivo* [31]. As shown in Fig. 5, addition of Iban was found to reduce the probability of BK_{Ca} channels taken in these cells. However, the magnitude of Iban-mediated inhibition of BK_{Ca}-channel activity did not differ significantly in membrane stretch created with −2, −4 and −6 kPa (Fig. 5B).

3.8. Effect of Iban and oxalate on the activity of BK_{Ca} channels

Oxalate was previously reported to interact with Ca^{2+} in renal tubular cells, and nitrogen-containing bisphosphonates could prevent the formation of calcium oxalate stone [1,7,26,34]. As such, we intended to explore whether the inhibitory effects of Iban and oxalate on these channels can operate to be additive. Of interest, as shown in Fig. 6, Iban (10 μM) produced a reduction of the channel open probability measured at the level of +50 mV; however, a subsequent addition of oxalate (30 μM) did not decrease channel activity further. Oxalate (30 μM) alone significantly reduced the probability of BK_{Ca}-channel openings from 0.192 ± 0.015 to 0.082 ± 0.008 (n = 12, P < 0.05). There was no significant difference in the channel open probability between the presence of Iban alone and Iban plus oxalate (0.084 ± 0.009 [n = 13] *versus* 0.082 ± 0.012 [n = 11], P > 0.05). These results thus indicate that the inhibition action by Iban and oxalate of single BK_{Ca} channels in MDCK cells is not additive.

3.9. Inhibitory effect of Iban, TRAM-34, Iban plus DC-EBIO and Iban plus 9-phenanthrol (9-PA) on the activity of intermediate-conductance Ca^{2+}-activated K^+ (IK_{Ca}) channels in MDCK cells

Earlier work in our laboratory has shown the inhibitory effects of Iban on IK_{Ca}-channel activity in RAW 264.7 osteoclast precursor cells [45]. In another set of experiments, we further assessed whether the activity of IK_{Ca} channels in MDCK cells can be sensitive to any change in the presence of Iban. As shown in Fig. 7, during cell exposure to Iban at a concentration of 30 and 100 μM, the probability of IK_{Ca}-channel openings were drastically decreased, although this compound was unable to modify single-channel amplitude. Similarly, TRAM-34 (3 μM), an inhibitor of IK_{Ca} channels, was effective at suppressing the activity of IK_{Ca} channels. Iban-induced reduction of IK_{Ca} channels was reversed by further addition of either DC-EBIO or 9-phenanthrol. Both DC-EBIO and 9-phenanthrol were reported to activate IK_{Ca} channels [8,35,45]. Therefore, the present results showing the Iban's ability to suppress IK_{Ca}-channel activities are consistent with our previous report made in RAW 264.7 cells [45].

3.10. Effect of Iban, Iban plus PF573228, and Iban plus DC-EBIO on membrane potential in MDCK cells

To determine whether Iban has any effects on the membrane potential of MDCK cells, a final set of experiments were conducted under current-clamp recordings. Cells, bathed in normal Tyrode's solution containing 1.8 mM $CaCl_2$, had a resting potential of −58.4 ± 2.6 mV (n = 19). When MDCK cells were exposed to Iban (30 μM), the membrane potential became progressively depolarized to −52.1 ± 2.8 mV (n = 13, P < 0.05) (Fig. 8). Subsequent application of PF573228 (10 μM) reversed Iban-mediated depolarization as evidenced by membrane hyperpolarization back to −56.1 ± 2.4 mV (n = 12, P < 0.05). Similarly, in continued presence of Iban (30 μM), a further addition of DC-EBIO hyperpolarized the cells back to −56.3 ± 2.6 mV (n = 11, P < 0.05). The typical effects of Iban, Iban plus PF573228 and Iban plus DC-EBIO on changes in membrane potential in MDCK cells are illustrated in Fig. 8A. These results reflect that Iban-mediated membrane depolarization seen in MDCK cells can result primarily from its inhibition of BK_{Ca} or/and IK_{Ca} channels. The inhibitory action on the activity of both BK_{Ca} and IK_{Ca} channels may cause membrane depolarization, thereby affecting functional activities of renal tubular cells, if this action occurring in native cells is the same as that shown here.

4. Discussion

In this study, the single-channel conductance of BK_{Ca} channels measured with the use of 145 mM K^+ on both sides of the membrane in MDCK was 198 ± 12 pS (n = 15). This value is similar to those of typical BK_{Ca} channels described previously in different cell types [5,11], but much greater than those of small- or intermediate-conductance Ca^{2+}-activated K^+ channels. Moreover, the channel activity presented here is sensitive to stimulation by membrane depolarization, $[Ca^{2+}]_i$ and membrane stretch, and it can be blocked by paxilline or ketamine.

A previous study showed that H_2S donor could prevent gastric damage caused by alendronate, another bisphosphonate [25]. Consistent with previous studies [5], our results demonstrated the ability of NaHS/H_2S to counteract Iban-mediated decrease of both macroscopic I_K amplitude and BK_{ca}-channel activity recorded from MDCK cells. H_2S has been reported to protect the kidney against different forms of injury [16]. Therefore, this volatile molecule

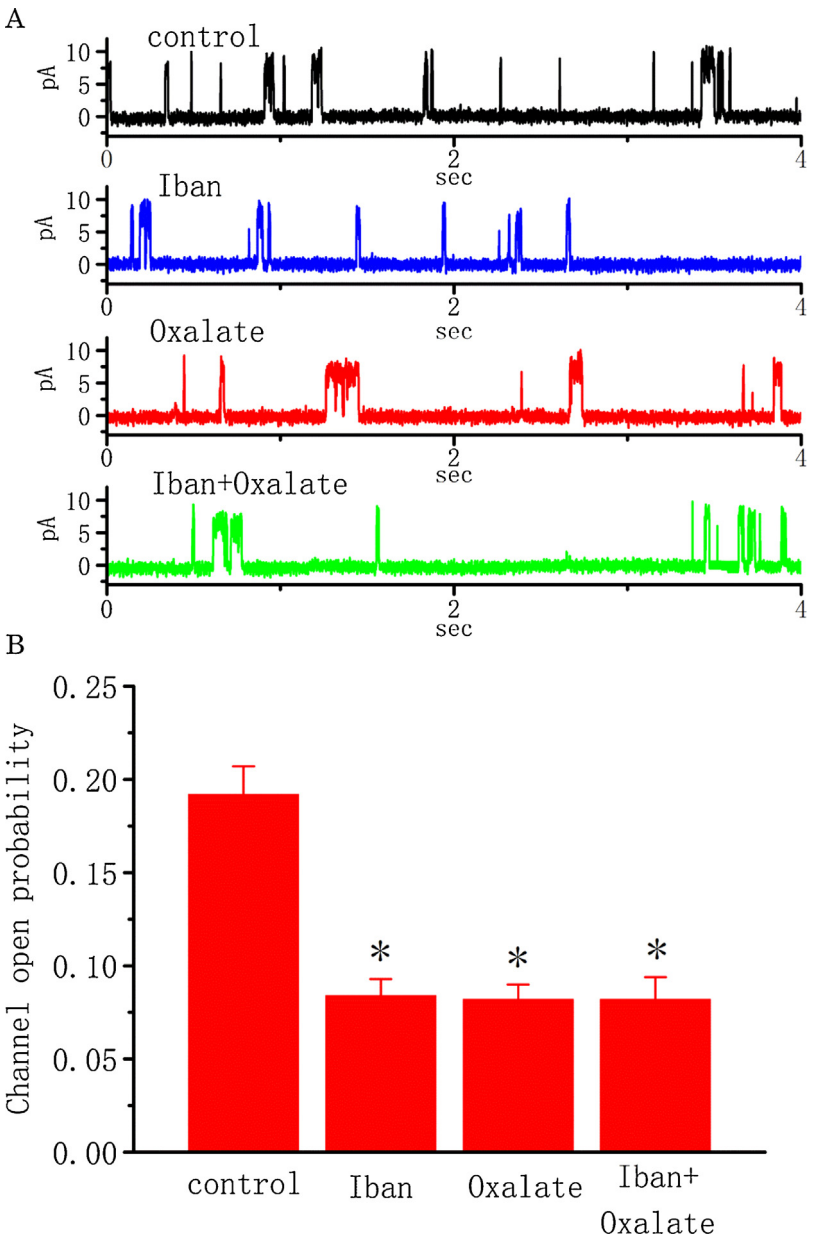

Fig. 6. Inhibitory effects of Iban and oxalate on the activity of BK_{Ca} channels recorded from MDCK cells. The experiments were conducted in symmetrical K^+ solution (145 mM) containing 1.8 mM $CaCl_2$, and the channels were recorded from cell-attached patched of MDCK cells. The potential was held at +50 mV. (A) Original current traces obtained in control (black) or during the exposure to 10 μM Iban (blue), 30 μM oxalate (red), or 10 μM Iban plus 30 μM oxalate (green). (B) Bar graph showing the effect of Iban (10 μM) and oxalate (30 μM) on the probability of BK_{Ca}-channel openings. Values are means ± SEM for $n = 11–13$ cells in each group. In the experiments with Iban plus oxalate, oxalate was subsequently applied after addition of Iban to the bath. *Significantly different from control ($P < 0.05$). (For interpretation of the references to color in this figure legend, the reader is referred to the web version of this article.)

may protect the damage by bisphosphonates of renal epithelium through a mechanism linked to activation of BK_{Ca} channels.

Numerous reports have demonstrated that ketamine, a recreational drug owing to its anesthetic and hallucinogenic actions, could produce significant nephrotoxicity [4,6,12,33,39]. In this study, this agent was noted to suppress I_K amplitude, and its effect could ascribe from its suppression of BK_{Ca} channels as reported previously [11]. Whether ketamine-induced tubular cell necrosis or obstructive uropathy described previously [4,6,12,33,39] is associated with an inhibition of BK_{Ca} channels remain to be further studied. Moreover, the administration of bisphosphonates would potentially exacerbate ketamine-mediated damage, because both agents suppress the activity of BK_{Ca} channels in renal tubular cells or smooth muscle cells of a urinary bladder. Meanwhile, in continued presence of Iban, oxalate-induced inhibition of BK_{Ca} channels seen in MDCK was abolished, suggesting that these two agents may work through a similar mechanism. Our results are in agreement with a number of studies reporting that bisphosphonates have a preventive role in the formation of calcium oxalate stones [1,7,26,30,34].

In the present study, the ability of Iban to produce an apparent shift of 22 mV to a positive potential in the activation curve of BK_{Ca} channels in MDCK cells was observed without any changes in the gating charge of this curve for the opening of BK_{Ca} channels. It is thus possible that its interaction with BK_{Ca} channels is not mediated through a direct effect on voltage sensor *per se*. Unlike its effects on IK_{Ca} channels [45], the binding site of Iban is most likely

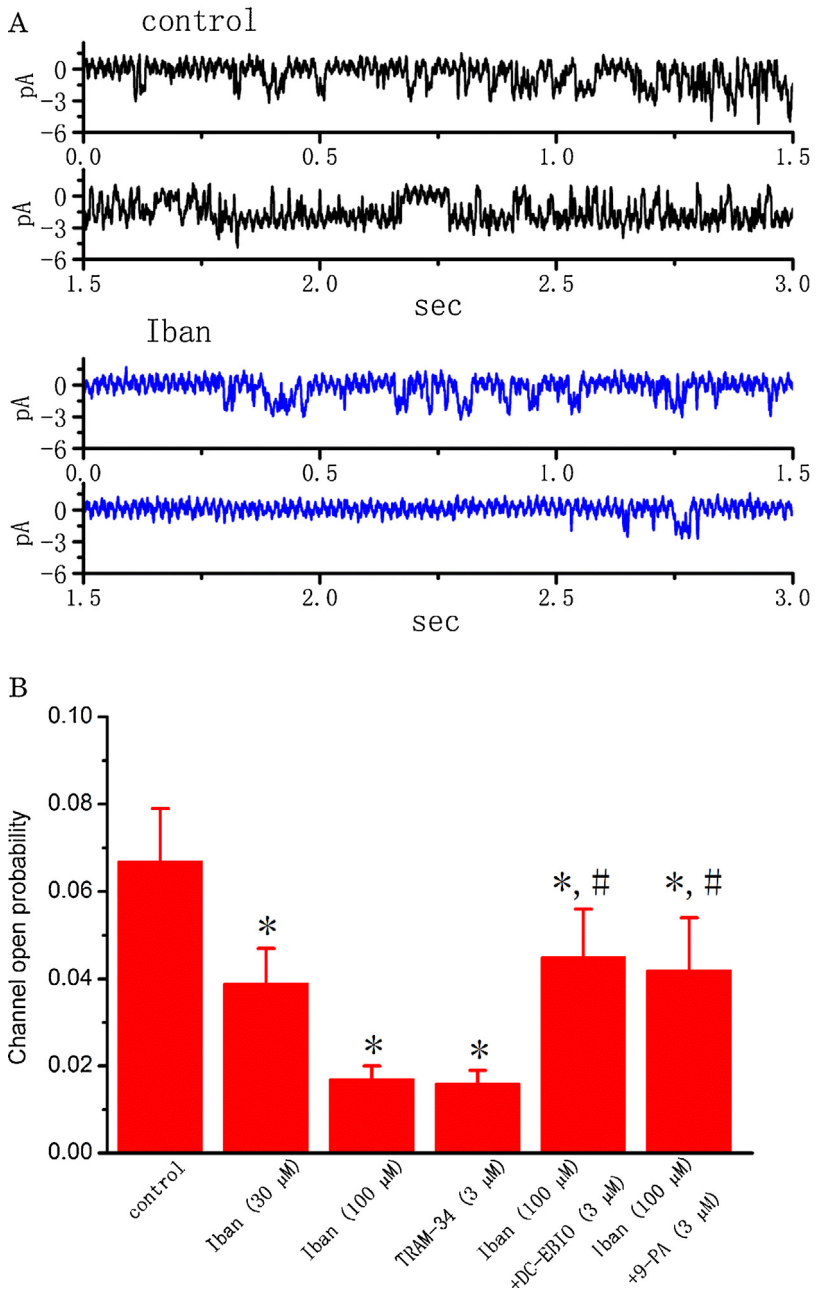

Fig. 7. Effects of Iban on the activity of IK_{Ca} channels recorded from MDCK cells. In these experiments, cells were immersed in normal Tyrode's solution containing 1.8 mM $CaCl_2$, and the holding potential was set at 0 mV relative to the bath when the recording pipette with filled with K^+-containing solution. (A) Original traces of IK_{Ca} channels obtained in control (upper, black) and after addition of 100 μM Iban (lower, blue). Notably, unlike the activity of BK_{Ca} channels described above, downward deflection indicates the opening event of the IK_{Ca} channel. (B) Summary of the data showing effects of Iban, TRAM-34, Iban plus DC-EBIO, and Iban plus 9-phenanthrol on the probability of IK_{Ca}-channel openings in MDCK cells. Values are means ± SEM for $n = 10–13$ cells in each group. *Significantly different from control ($P < 0.05$) and #significantly ($P < 0.05$) different from Iban (100 μM) alone. 9-PA: 9-phenanthrol. (For interpretation of the references to color in this figure legend, the reader is referred to the web version of this article.)

to lie outside of the trans-membrane field. Our results also clearly showed that in MDCK cells, membrane stretch could enhance the activity of BK_{Ca} channels, despite inability of this maneuver to alter the single-channel conductance of these channels during such maneuver. The BK_{Ca} channel in MDCK cells thus indeed exhibits a mechano-sensitive property as described previously [5,36,44,46]. These data suggest that the BK_{Ca} channel may play a role in stretch-, volume- or flow-dependent cellular effects in renal tubular cells *in vivo* [17,31]. Iban could decrease the probability of BK_{Ca}-channel openings in MDCK cells as well as modify the Ca^{2+} sensitivity of BK_{Ca} channels. The results reflect that this compound can exert its effect via a decrease in the affinity of Ca^{2+} ions for Ca^{2+} binding site in the membrane. Therefore, during an increase in tensile strength of renal tubule, membrane depolarization, changes in resting $[Ca^{2+}]_i$, and membrane stretch may synergistically contribute to the opening of BK_{Ca} channels enriched in renal tubular cells, which are sensitive to inhibition by Iban or other bisphosphonates.

On the basis of a minimal reaction scheme, the *K*D value of Iban required for Iban-induced shortening in the slow component of mean open time measured from BK_{Ca} channels is 12.2 μM. This value is lower than that used to suppress the activity of IK_{Ca} channel in RAW 264.7 cells [45]. Both decreased I_K amplitude and membrane depolarization caused by this agent in renal tubular cells can be dependent not only on the Iban concentration, but also on the pre-existing membrane potential, $[Ca^{2+}]_i$, and membrane stretch. The estimated peak of plasma Iban concentration has been reported

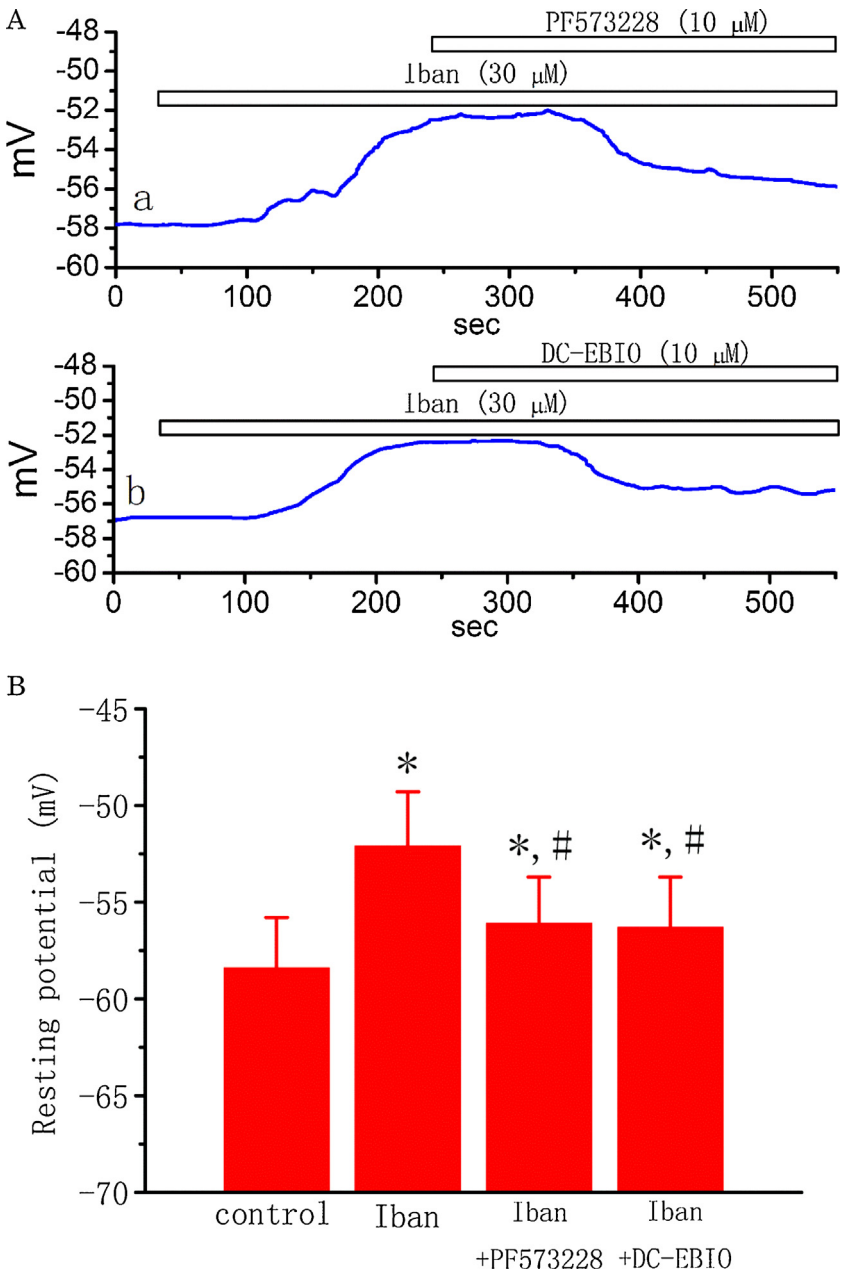

Fig. 8. Effects of Iban, Iban plus PF573228 and Iban plus DC-EBIO on membrane potential in MDCK cells. In current-clamp configuration, cells were bathed in normal Tyrode's solution containing 1.8 mM $CaCl_2$. (Aa) Original potential trace showing effects of Iban (30 μM) and PF573228 (10 μM) on membrane potential. (Ab) Original potential trace showing effect of Iban (30 μM) and DC-EBIO (10 μM) on membrane potential. (B) Summary of the data showing effect of Iban, Iban plus PF573228, and Iban plus DC-EBIO on membrane potential of MDCK cells. Values are means ± SEM for $n = 11–15$ cells in each group. *Significantly different from control ($P < 0.05$) and #significantly ($P < 0.05$) different from Iban (30 μM) alone.

to reach 5×10^3 ng/ml (around 14 μM) [21]. Additionally, the bisphosphonates like Iban can be virtually taken or even accumulated in renal tubular cells through the process of fluid phase endocytosis [3,38]. Consequently, the observed effects by Iban on BK_{Ca} channels tend to develop during the open state of the channel and may occur at the range of the concentrations achievable in humans.

In this study, we were unable to detect voltage-gated Na^+ or Ca^{2+} currents in MDCK cells. Distinguished from previous reports made in thyroid and breast cancer cells and [20,48], addition of Iban at a concentration of 10 μM did not produce any change in the level of $[Ca^{2+}]_i$ in MDCK cells, nor did it enhance BK_{Ca}-channel activity. No clear difference in acute nephrotoxicity caused by zolendronate and Iban was reported [18]. Iban at higher concentrations also virtually suppressed the activity of IK_{Ca} channels in MDCK cells, and DC-EBIO or 9-phenanthrol counteracted Iban-induced suppression of these channels. Therefore, it seems unlikely that Iban-mediated inhibition of BK_{Ca}- or IK_{Ca}-channel activity in renal tubular cells results predominantly from sustained elevation of $[Ca^{2+}]_i$.

In renal epithelial cells, K^+ recycling is an essential step in the control of trans-epithelial transport. Any activation of K_{Ca} channels would enhance K^+ recycling, hyperpolarize the membrane potential, and facilitate the transport of other ions (*e.g.*, Na^+ and Ca^{2+} ions) or solutes [24,40,41,44]. In addition to inhibition of farnesyl pyrophosphate synthase [19], the inhibitory effects of Iban on these channels may significantly contribute to the underlying mechanisms by which it and other structurally related bisphosphonates affect functional activities of renal epithelial cells, assuming that similar findings can occur *in vivo*. Whether the nephrotoxicity caused by chronic treatment with Iban occurring *in vivo* is linked to its effects on ion-channel activity needs to be further investigated.

Conflict of interest

No conflicts of interest, financial or otherwise, are declared by the author(s).

Acknowledgements

The authors would like to thank Yu-Kai Liao and Ching-An Kao for contributing to part of the earlier experiments. This study was partly supported by National Cheng Kung University (no. 1030101), Tainan City, Taiwan. Hui-Zen Chen received a student fellowship from National Cheng Kung University, Tainan City, Taiwan.

References

[1] E.K. Basok, A. Basaran, N. Atsu, A. Yildirim, R. Tokuc, Are new-generation bisphosphonates effective for the inhibition of calcium oxalate stone formation in a rat model? Urol. Int. 81 (2008) 325–329.
[2] R. Bergner, B. Siegrist, N. Gretz, G. Pohlmeyer-Esch, B. Kränzlin, Nephrotoxicity of ibandronate and zoledronate in Wister rats with normal renal function and after unilateral nephrectomy, Pharmacol. Res. 99 (2015) 16–22.
[3] R. Bergner, B. Siegrist, B. Kränzlin, N. Gretz, H. Faust, T. Pfister, Determination of renal tissue ibandronate levels in rats with normal and mildly impaired renal function, J. Pharm. Toxicol. Meth. 68 (2013) 225–230.
[4] C.L. Chen, T.L. Cha, S.T. Wu, S.H. Tang, C.W. Tsao, E. Meng, Renal infarction secondary to ketamine abuse, Am. J. Emerg. Med. 31 (3–5) (2013) 1153.
[5] N.J. Chiang, S.N. Wu, L.T. Chen, The potent activation of Ca^{2+}-activated K^+ current by NVP-AUY922 in the human pancreatic duct cell line (PANC-1) possibly independent of heat shock protein 90 inhibition, J. Pharmacol. Sci. 127 (2015) 404–413.
[6] P.I. Dargan, H.C. Tang, W. Liang, D.M. Wood, D.T. Yew, Three months of methoxetamine administration is associated with significant bladder and renal toxicity in mice, Clin. Toxicol. (Phila) 52 (2014) 176–180.
[7] S. Ebisuno, Y. Kohjimoto, M. Nishikawa, T. Inagaki, T. Komura, T. Ohkawa, Effect of etidronate disorium on crystallizations in synthetic urine and calcium oxalate crystal adhesion to Madin–Darby canine kidney (MDCK) cells, Int. J. Urol. 5 (1998) 582–587.
[8] C.J. Garland, S.V. Smirnov, P. Bagher, C.S. Lim, C.Y. Huang, R. Mitchell, C. Stanley, A. Pinkney, K.A. Dora, TRPM4 inhibitor 9-phenanthrol activates endothelial cell intermediate conductance calcium-activated potassium channels in rat isolated mesenteric artery, Br. J. Pharmacol 172 (2015) 1114–1123.
[9] P.R. Grimm, R.M. Foutz, R. Brenner, S.C. Sansom, Identification and localization of BK-b subunits in the distal neprhon of the mouse kidney, Am. J. Physiol. Renal Physiol. 293 (2007) F350–359.
[10] C. Huang, C.A. Pollock, X.M. Chen, Role of the potassium channel KCa3.1 in diabetic nephropathy, Clin. Sci. (Lond) 127 (2014) 423–433.
[11] M.H. Huang, K.H. Lin, S.J. Chen, A.Y. Shen, F.T. Wu, S.N. Wu, Effects of ketamine and its metabolites on ion currents in differentiated hippocampal H19-7 neuronal cells and in HEK293T cells transfected with a-hslo subunit, Neurotoxicology 33 (2012) 1058–1066.
[12] P.W. Huang, E. Meng, T.L. Char, G.H. Sun, D.S. Yu, S.Y. Chang, 'Walking-stick ureters' in ketamine abuse, Kidney Int. 80 (2011) 895.
[13] C.R. Jan, W.C. Chen, S.N. Wu, C.J. Tseng, Nifedipine: verapamil and diltiazem block shock-wave-induced rises in cytosolic calcium MDCK cells, Chin. J. Physiol. 41 (1998) 181–188.
[14] C.R. Jan, S.N. Wu, C.J. Tseng, The ether lipid ET-18-OCH3 increases cytosolic Ca^{2+} concentrations in Madin Darby canine kidney cells, Br. J. Pharmacol. 127 (1999) 1502–1510.
[15] I. Kino, Y. Kato, J.H. Lin, Y. Sugiyama, Renal handling of biphosphonate alendronate in rats, Biopharm. Drug Dispos. 20 (1999) 193–198.
[16] A.M. Koning, A.R. Frenay, H.G. Leuvenink, H. van Goor, Hydrogen sulfide in renal physiology, disease and transplantation—the smell of renal protection, Nitric Oxide 46 (2015) 37–49.
[17] W. Liu, C. Schreck, R.A. Coleman, J.B. Wade, Y. Hernandez, B. Zavilowitz, R. Warth, T.R. Kleyman, L.M. Satlin, Role of NKCC in BK channel-mediated net K^+ secretion in the CCD, Am. J. Physiol. Renal Physiol. 301 (2011) F1088–F1097.
[18] D.W. Luedders, J. Steinhoff, M. Thill, A. Rody, M.K. Bohlmann, Lack of difference in acute nephrotoxicity of intravenous bisphosphonates zoledronic acid and ibandronate in women with breast cancer and bone metastases, Anticancer Res. 35 (2015) 1797–1802.
[19] A. Luhe, K.P. Kunkele, M. Haiker, K. Schad, C. Zihlmann, F. Bauss, L. Suter, T. Pfister, Preclinical evidence for nitrogen-containing bisphosphonate inhibition of farnesyl diphosphate (FPP) synthase in the kidney: implications for renal safety, Toxicol. In Vitro 22 (2008) 899–909.
[20] Y.G. Ma, W.C. Liu, S. Dong, C. Du, X.J. Wang, J.S. Li, X.P. Xie, L. Wu, D.C. Ma, Z.B. Yu, M.J. Xie, Activation of BKCa channels in zoledronic acid-induced apoptosis of MDA-MB-231 breast cancer cells, PLoS One 7 (2012) e37451.
[21] D.D. Marathe, A. Marathe, D.E. Mager, Integrated model for denosumab and ibandronate pharmacodynamics in postmenopausal women, Biopharm. Drug Dispos. 32 (2011) 471–481.
[22] G.S. Markowitz, P.L. Fine, J.I. Stack, C.L. Kunis, J. Radhakrishnan, W. Palecki, J. Park, S.H. Nasr, S. Hoh, D.S. Siegel, V.D. D'Agati, Toxic acute tubular necrosis following treatment with zoledronate (Zometa), Kidney Int. 64 (2003) 281–289.
[23] L. Mosekilde, P. Vestergaard, L. Rejnmark, The pathogenesis, treatment and prevention of osteoporosis in men, Drugs 73 (2013) 15–29.
[24] F. Najjar, H. Zhou, T. Morimoto, J.B. Bruns, H.S. Li, W. Liu, T.R. Kleyman, L.M. Satlin, Dietary K+ regulates apical membrane expression of maxi-K channels in rabbit cortical collecting duct, Am. J. Physiol. Renal Physiol. 289 (2005) F922–F932.
[25] L.A. Nicolau, R.O. Silva, S.R. Damasceno, N.S. Carvalho, N.R. Costa, K.S. Aragão, A.L. Barbosa, P.M. Soares, M.H. Souza, J.V. Medeiros, The hydrogen sulfide donor, Lawesson's reagent, prevents alendronate-induced gastric damage in rats, Braz. J. Med. Biol. Res. 46 (2013) 708–714.
[26] A. Okada, H. Ohshima, Y. Itoh, T. Yasui, K. Tozawa, K. Kohri, Risk of renal stone formation induced by long-term bed rest could be decreased by premedication with bisphosphonate and increased by resistive exercise, Int. J. Urol. 15 (2008) 630–635.
[27] M.A. Perazella, G.S. Markowitz, Bisphosphonate nephrotoxicity, Kidney Int. 74 (2008) 1385–1393.
[28] T. Pfister, E. Atzpodien, B. Bohrmann, F. Bauss, Acute renal effects of intravenous bisphosphonates in the rat, Basic Clin. Pharmacol. Toxicol 97 (2005) 374–381.
[29] T. Pfister, E. Atzpodien, F. Bauss, The renal effects of minimally nephrotoxic doses of ibandronate and zoledronate following single and intermittent intravenous administration in rats, Toxicology 191 (2003) 159–167.
[30] P.A. Price, J.R. Buckley, M.K. Williamson, The amino bisphosphonate ibandronate prevents vitamin D toxicity and inhibits vitamin D-induced calcification of arteries, cartilage, lungs and kidneys in rats, J. Nutr. 131 (2001) 2910–2915.
[31] T. Rieg, V. Vallon, M. Sausbier, U. Sausbier, B. Kaissling, P. Ruth, H. Osswald, The role of the BK channel in potassium homeostasis and flow-induced renal potassium excretion, Kidney Int. 72 (2007) 566–573.
[32] I. Sehitoglu, L. Tumkaya, R. Bedir, Y. Kalkan, M.C. Cure, A.F. Yucel, O.U. Zorba, S. Yuce, E. Cure, Zoledronic acid aggravates kidney damage during ischemia reperfusion injury in rat, J. Environ. Pathol. Toxicol. Oncol. 34 (2015) 53–61.
[33] N.M. Selby, J. Anderson, P. Bungay, L.J. Chesterton, N.V. Kolhe, Obstructive nephropathy and kidney injury associated with ketamine abuse, NDT Plus 5 (2008) 310–312.
[34] H. Senzaki, T. Yasui, A. Okada, Y. Ito, K. Tozawa, K. Kohri, Alendronate inhibits urinary calcium microlith formation in a three-dimensional culture model, Urol. Res. 32 (2004) 223–228.
[35] A.Y. Shen, J.H. Tsai, H.C. Teng, M.H. Huang, S.N. Wu, Inhibition of intermediate-conductance Ca^{2+}-activated K^+ channel and cytoprotective properties of 4-piperidinomethyl-2-isopropyl-5-methylphenol, J. Pharm. Pharmacol. 59 (2007) 679–685.
[36] S.J. Sheu, S.N. Wu, D.N. Hu, Stretch-stimulated activity of large conductance calcium-activated potassium channels in human retinal pigment epithelial cells, J. Ocul. Pharmacol. Ther. 21 (2005) 429–435.
[37] E.C. So, K.C. Wu, C.H. Liang, J.Y. Chen, S.N. Wu, Evidence for activation of BKCa channels by a known inhibitor of focal adhesion kinase, PF573228, Life Sci. 89 (2011) 691–701.
[38] A. Verhulst, S. Sun, C.E. McKenna, P.C. D'Haese, Endocytotic uptake of zoledronic acid by tubular cells may explain its renal effects in cancer patients receiving high doses of the compound, PLoS One 10 (2015) e0121861.
[39] M.S. Wai, W.M. Chan, A.Q. Zhang, Y. Wu, D.T. Yew, Long-term ketamine and ketamine plus alcohol treatments produced damages in liver and kidney, Hum. Exp. Toxicol. 31 (2012) 877–886.
[40] P.A. Weling, Regulation of renal potassium secretion: molecular mechanisms, Semin. Nephrol. 33 (2013) 215–228.
[41] D. Wen, R.J. Cornelius, S.C. Sansom, Interacting influence of diuretics and diet on BK channel-regulated K homeostasis, Curr. Opin. Pharmacol. 15 (2014) 28–32.
[42] C.B. Woda, A. Bragin, T.R. Kleyman, L.M. Satin, Flow-dependent K^+ secretion in the cortical collecting duct is mediated by a maxi-K channel, Am. J. Physiol. Renal Physiol. 280 (2001) F786–F793.
[43] S.N. Wu, Large-conductance Ca^{2+}-activated K^+ channels: physiological role and pharmacology, Curr. Med. Chem. 10 (2003) 649–661.
[44] S.N. Wu, B.S. Chen, C.L. Hsu, T.I. Hsu, The large-conductance Ca^{2+}-activated K^+ channels: a target for the modulators of estrogen receptors, Curr. Top. Biochem. Res. 10 (2008) 93–101.
[45] S.N. Wu, Y.M. Huang, Y.K. Liao, Effects of ibandronate sodium, a nitrogen-containing bisphosphonate, on intermediate-conductance calcium-activated potassium channels in osteoclast precursor cells (RAW 264.7), J. Membr. Biol. 248 (2015) 103–115.
[46] S.N. Wu, P.H. Lin, K.S. Hsieh, Y.C. Liu, H.T. Chiang, Behavior of nonselective cation channels and large-conductance Ca^{2+}-activated K^+ channels induced by dynamic changes in membrane stretch in cultured smooth muscle cells of human coronary artery, J. Cardiovasc. Electrophysiol. 14 (2003) 44–51.
[47] S.N. Wu, A.Z. Wu, R.J. Sung, Identification of two types of ATP-sensitive K^+ channels in rat ventricular myocytes, Life Sci. 80 (2007) 378–387.
[48] D.M. Yang, C.W. Chi, H.M. Chang, L.H. Wu, T.K. Lee, J.D. Lin, S.T. Chen, C.H. Lee, Effects of clodronate on cancer growth and Ca^{2+} signaling of human thyroid carcinoma cell lines, Anticancer Res. 24 (3a) (2004) 1617–1623.